

The QGP dynamics in relativistic heavy-ion collisions

E. L. Bratkovskaya^{1,2}, W. Cassing³, V. P. Konchakovski^{3,4},
O. Linnyk³, V. Ozvenchuk², V.D. Toneev^{5,2} and V. Voronyuk^{5,2,4}

¹ Institute for Theoretical Physics, University of Frankfurt, Frankfurt, Germany

² Frankfurt Institute for Advanced Study, Frankfurt, Germany

³ Institute for Theoretical Physics, University of Giessen, Giessen, Germany

⁴ Bogolyubov Institute for Theoretical Physics, Kiev, Ukraine

⁵ Joint Institute for Nuclear Research, Dubna, Russia

Abstract. The dynamics of partons and hadrons in relativistic nucleus-nucleus collisions is analyzed within the novel Parton-Hadron-String Dynamics (PHSD) transport approach, which is based on a dynamical quasiparticle model for the partonic phase (DQPM) including a dynamical hadronization scheme. The PHSD model reproduces a large variety of observables from SPS to LHC energies, e.g. the quark-number scaling of elliptic flow, transverse mass and rapidity spectra of charged hadrons, dilepton spectra, open and hidden charm production, collective flow coefficients etc., which are associated with the observation of a sQGP. The 'highlights' of the latest results on collective flow are presented and open questions/perspectives are discussed.

1. Introduction

The dynamics of the early universe in terms of the 'Big Bang' may be studied experimentally by ultrarelativistic nucleus-nucleus collisions at Relativistic-Heavy-Ion-Collider (RHIC) or Large-Hadron-Collider (LHC) energies in terms of 'tiny bangs' in the laboratory. The Power Spectrum extracted from the Cosmic Microwave Background Radiation has some analogy to the Fourier components of particles in the azimuthal angular distribution [1]. The discovery of large azimuthal anisotropic flow at RHIC has provided conclusive evidence for the creation of dense partonic matter in ultra-relativistic nucleus-nucleus collisions. With sufficiently strong parton interactions, the medium in the collision zone can be expected to achieve local equilibrium and exhibit approximately hydrodynamic flow [2, 3, 4]. The momentum anisotropy is generated due to pressure gradients of the initial "almond-shaped" collision zone produced in noncentral collisions [2, 3]. The azimuthal pressure gradient extinguishes itself soon after the start of the hydrodynamic evolution, so the final flow is only weakly sensitive to later stages of the fireball evolution. The pressure gradients have to be large enough to translate an early asymmetry in density of the initial state to a final-state momentum-space anisotropy. In these collisions a new state of strongly interacting matter is created, being characterized by a very low shear viscosity η to entropy density s ratio, η/s , close to a nearly perfect fluid [5, 6, 7]. Lattice QCD (lQCD) calculations [8, 9] indicate that a crossover region between hadron and quark-gluon matter should have been reached in these experiments.

An experimental manifestation of this collective flow is the anisotropic emission of charged particles in the plane transverse to the beam direction. This anisotropy is described by the different flow parameters defined as the proper Fourier coefficients v_n of the particle distributions in azimuthal angle ψ with respect to the reaction plane angle Ψ_{RP} . At the highest RHIC collision



energy of $\sqrt{s_{NN}} = 200$ GeV, differential elliptic flow measurements $v_2(p_T)$ have been reported for a broad range of centralities or number of participants N_{part} . For N_{part} estimates, the geometric fluctuations associated with the positions of the nucleons in the collision zone serve as the underlying origin of the initial eccentricity fluctuations. These data are found to be in accord with model calculations that an essentially locally equilibrated quark gluon plasma (QGP) has little or no viscosity [10, 11, 12]. Collective flow continues to play a central role in characterizing the transport properties of the strongly interacting matter produced in heavy-ion collisions at RHIC and even LHC and shed some light on the scale of initial state fluctuations.

The Beam-Energy-Scan (BES) program proposed at RHIC [13] covers the energy interval from $\sqrt{s_{NN}} = 200$ GeV, where partonic degrees of freedom play a decisive role, down to the AGS energy of $\sqrt{s_{NN}} \approx 5$ GeV, where most experimental data may be described successfully in terms of hadronic degrees-of-freedom, only. Lowering the RHIC collision energy and studying the energy dependence of anisotropic flow allows to search for the possible onset of the transition to a phase with partonic degrees-of-freedom at an early stage of the collision as well as possibly to identify the location of the critical end-point that terminates the cross-over transition at small quark-chemical potential to a first order phase transition at higher quark-chemical potential [14, 15].

This contribution aims to summarize excitation functions for different harmonics of the charged particle anisotropy in the azimuthal angle at midrapidity in a wide transient energy range, *i.e.* from the AGS to the top RHIC energy. The first attempts to explain the preliminary STAR data with respect to the observed increase of the elliptic flow v_2 with the collision energy have failed since the traditional available models did not allow to clarify the role of the partonic phase [16]. In this contribution we investigate the energy behavior of different flow coefficients, their scaling properties and differential distributions (cf. Ref. [17, 18]). Our analysis of the STAR/PHENIX RHIC data – based on recent results of the BES program – will be performed within the Parton-Hadron-String Dynamics (PHSD) transport model [19] that includes explicit partonic degrees-of-freedom as well as a dynamical hadronization scheme for the transition from partonic to hadronic degrees-of-freedom and vice versa. For more detailed descriptions of PHSD and its ingredients we refer the reader to Refs. [20, 21, 22, 23].

2. Results for collective flows

We directly continue with the results from PHSD in comparison with other approaches and the available experimental data.

2.1. Elliptic flow

The largest component, known as elliptic flow v_2 , is one of the early observations at RHIC [24]. The elliptic flow coefficient is a widely used quantity characterizing the azimuthal anisotropy of emitted particles,

$$v_2 = \langle \cos(2\psi - 2\Psi) \rangle = \langle \frac{p_x^2 - p_y^2}{p_x^2 + p_y^2} \rangle, \quad (1)$$

where Ψ_{RP} is the azimuth of the reaction plane, p_x and p_y are the x and y component of the particle momenta and the brackets denote averaging over particles and events. This coefficient can be considered as a function of centrality, pseudorapidity η and/or transverse momentum p_T . We note that the reaction plane in PHSD is given by the $(x - z)$ plane with the z -axis in beam direction. The reaction plane is defined as a plane containing the beam axes and the impact parameter vector.

We recall that at high bombarding energies the longitudinal size of the Lorentz contracted nuclei becomes negligible compared to its transverse size. The forward shadowing effect then becomes negligible and the elliptic flow fully develops in-plane, leading to a positive value of

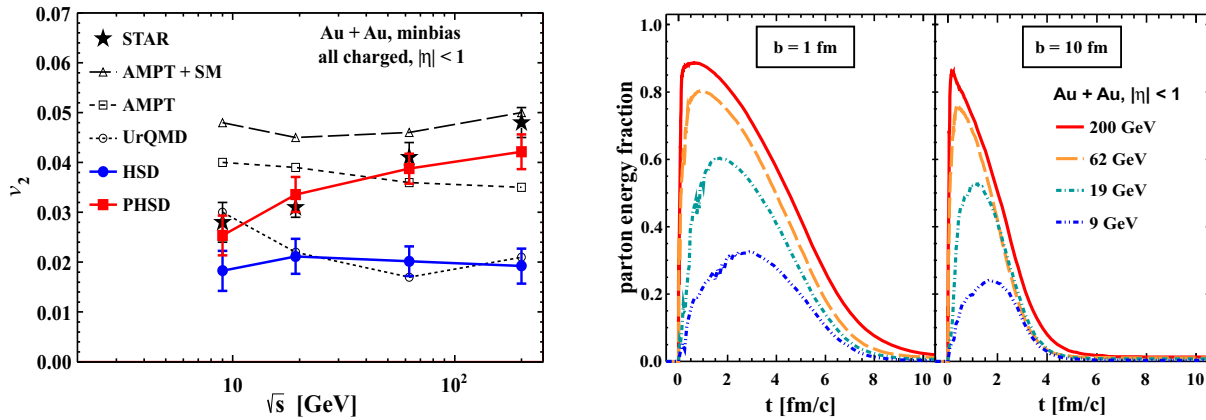


Figure 1. (l.h.s.) The average elliptic flow v_2 of charged particles at midrapidity for minimum bias collisions at $\sqrt{s_{NN}} = 9.2, 19.6, 62.4$ and 200 GeV (stars) is taken from the data compilation of Ref. [16]). The corresponding results from different models are compared to the data and explained in more detail in the text. (r.h.s.) Evolution of the parton fraction of the total energy density at midrapidity (from PHSD) for different collision energies at impact parameters $b = 1$ fm and 10 fm.

the average flow v_2 since no shadowing from spectators takes place. In Fig. 1 (l.h.s.) the experimental v_2 data compilation for the transient energy range is compared to the results from various models: PHSD, HSD as well as from UrQMD and AMPT as included in Ref. [16]. The centrality selection is the same for the data and the various models.

The HSD [27, 28, 29] and UrQMD (Ultra relativistic Quantum Molecular Dynamics) [25, 26] are the hadron-string models and, thus, essentially provide information on the contribution from the hadronic phase [30]. As seen in Fig. 1, being in agreement with data at the lowest energy $\sqrt{s_{NN}} = 9.2$ GeV, the HSD and UrQMD model results then either remain approximately constant or decrease slightly with increasing $\sqrt{s_{NN}}$ and do not reproduce the rise of v_2 with the collision energy as seen experimentally.

The AMPT (A Multi Phase Transport model) [31, 32] uses initial conditions of a perturbative QCD (pQCD) inspired model which produces multiple minijet partons according to the number of binary initial nucleon-nucleon collisions. The string melting (SM) version of the AMPT model (labeled in Fig. 1 as AMPT-SM) is based on the idea of 'melting' of hadrons or strings above the critical energy density of $\varepsilon \sim 1$ GeV/fm³ to massless partons. The subsequent scattering of the quarks are based on a parton cascade with (adjustable) effective cross sections which are significantly larger than those from pQCD [31, 32]. Once the partonic interactions terminate, the partons hadronize through the mechanism of parton coalescence.

We find from Fig. 1 that the interactions between the minijet partons in the AMPT model indeed increase the elliptic flow significantly as compared to the hadronic models UrQMD and HSD. An additional inclusion of interactions between partons in the AMPT-SM model gives rise to another 20% of v_2 bringing it into agreement (for AMPT-SM) with the data at the maximal collision energy. So, both versions of the AMPT model indicate the importance of partonic contributions to the observed elliptic flow v_2 but do not reproduce its growth with $\sqrt{s_{NN}}$. The authors address this result to the partonic-equation-of state (EoS) employed which corresponds to a massless and noninteracting relativistic gas of particles. This EoS deviates severely from the results of lattice QCD calculations for temperatures below $2-3 T_c$. Accordingly, the degrees-of-freedom are propagated without self-energies and a parton spectral function.

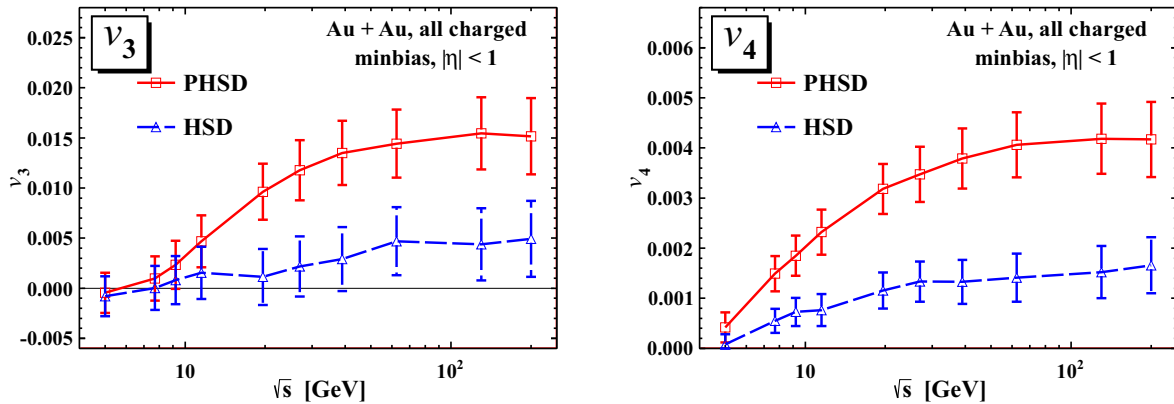


Figure 2. Average anisotropic flows v_3 (l.h.s.) and v_4 (r.h.s.) of charged particles at mid-pseudorapidity for minimum bias Au + Au collisions calculated within the PHSD (solid lines, red) and HSD (dashed lines, blue) models.

The PHSD approach incorporates the latter medium effects in line with a lQCD equation-of-state and also includes a dynamical hadronization scheme based on covariant transition rates. As has been demonstrated in Refs. [17, 18] and explicitly shown in Fig. 1 (l.h.s.), the elliptic flow v_2 from PHSD (red line) agrees with the data from the STAR collaboration and clearly shows an increase with bombarding energy.

An explanation for the increase in v_2 with collision energy is provided in Fig. 1 (r.h.s.) where the partonic fraction of the energy density is shown with respect to the total energy where the energy densities are calculated at mid-rapidity. As discussed above the main contribution to the elliptic flow is coming from an initial partonic stage at high \sqrt{s} . The fusion of partons to hadrons or, inversely, the melting of hadrons to partonic quasiparticles occurs when the local energy density is about $\varepsilon \approx 0.5$ GeV/fm³. As follows from Fig. 1, the parton fraction of the total energy goes down substantially with decreasing bombarding energy while the duration of the partonic phase is roughly the same. The maximal fraction reached is the same in central and peripheral collisions but the parton evolution time is shorter in peripheral collisions. One should recall again the important role of the repulsive mean-field for partons in the PHSD model that leads to an increase of the flow v_2 with respect to HSD predictions (cf. also Ref. [33]). We point out in addition that the increase of v_2 in PHSD relative to HSD is also partly due to the higher interaction rates in the partonic medium because of a lower ratio of η/s for partonic degrees-of-freedom at energy densities above the critical energy density than for hadronic media below the critical energy density [34, 35, 36]. The relative increase in v_3 and v_4 in PHSD essentially is due to the higher partonic interaction rate and thus to a lower ratio η/s in the partonic medium which is mandatory to convert initial spacial anisotropies to final anisotropies in momentum space [37].

2.2. Higher-order flow harmonics

Depending on the location of the participant nucleons in the nucleus at the time of the collision, the actual shape of the overlap area may vary: the orientation and eccentricity of the ellipse defined by the participants fluctuates from event to event. Note, however, that by averaging over many events an almond shape is regained for the same impact parameter.

Recent studies suggest that fluctuations in the initial state geometry can generate higher-order flow components [1, 10, 38, 39]. The azimuthal momentum distribution of the emitted

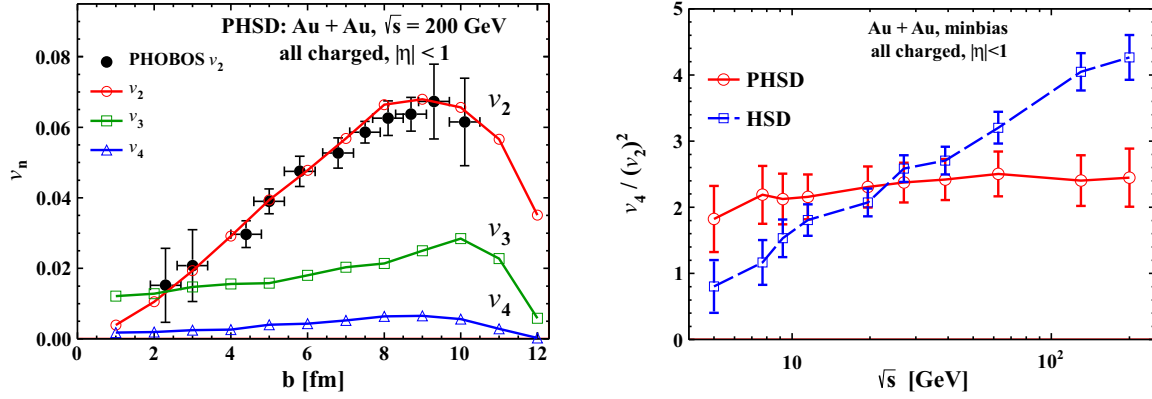


Figure 3. (l.h.s.) Impact parameter dependence of anisotropic flows of charged particles at mid-pseudorapidity for minimum bias collisions of Au+Au at $\sqrt{s_{NN}} = 200$ GeV. Experimental points are from Ref. [43]. (r.h.s.) Beam energy dependence of the ratio $v_4/(v_2)^2$ for Au+Au collisions. The solid and dashed curves are calculated within the PHSD and HSD models, respectively.

particles is commonly expressed in the form of a Fourier series as

$$E \frac{d^3N}{d^3p} = \frac{d^2N}{2\pi p_T dp_T dy} \left(1 + \sum_{n=1}^{\infty} 2v_n(p_T) \cos(n(\psi - \Psi_n)) \right), \quad (2)$$

where v_n is the magnitude of the n -th order harmonic term relative to the angle of the initial-state spatial plane of symmetry Ψ_n . The anisotropy in the azimuthal angle ψ is usually characterized by the even order Fourier coefficients with the reaction plane $\Psi_n = \Psi_{RP}$: $v_n = \langle \exp(in(\psi - \Psi_{RP})) \rangle$ ($n = 2, 4, \dots$), since for a smooth angular profile the odd harmonics vanish. For the odd components, e.g. v_3 , one should take into account event-by-event fluctuations with respect to the participant plane $\Psi_n = \Psi_{PP}$. We calculate the v_3 coefficients with respect to Ψ_3 as: $v_3\{\Psi_3\} = \langle \cos(3[\psi - \Psi_3]) \rangle / Res(\Psi_3)$. The event plane angle Ψ_3 and its resolution $Res(\Psi_3)$ are calculated as described in Ref. [40] via the two-sub-events method [41, 42].

In Fig. 2 we display the PHSD and HSD results for the anisotropic flows v_3 and v_4 of charged particles at mid-pseudorapidity for Au+Au collisions as a function of $\sqrt{s_{NN}}$. The pure hadronic model HSD gives $v_3 \approx 0$ for all energies. Accordingly, the results from PHSD (dashed red line) are systematically larger than from HSD (dashed blue line). Unfortunately, our statistics are not good enough to allow for more precise conclusions. The hexadecupole flow v_4 stays almost constant in the energy range $\sqrt{s_{NN}} \geq 10$ GeV; at the same time the PHSD gives noticeably higher values than HSD which we attribute to the higher interaction rate in the partonic phase.

Alongside with the integrated flow coefficients v_n the PHSD model reasonably describes their distribution over centrality or impact parameter b . A specific comparison at $\sqrt{s_{NN}} = 200$ GeV is shown in Fig. 3 for v_2 , v_3 and v_4 . While v_2 increases strongly with b up to peripheral collisions, v_3 and v_4 are only weakly sensitive to the impact parameter. The triangular flow is always somewhat higher than the hexadecupole flow in the whole range of impact parameters b .

2.3. Ratios of different harmonics

Different harmonics can be related to each other. In particular, hydrodynamics predicts that $v_4 \propto (v_2)^2$ [44]. The simplest prediction that $v_4 = 0.5(v_2)^2$ is given for a boosted thermal freeze-out distribution of an ideal fluid, Ref. [45]. In this work it was noted also that v_4 is largely

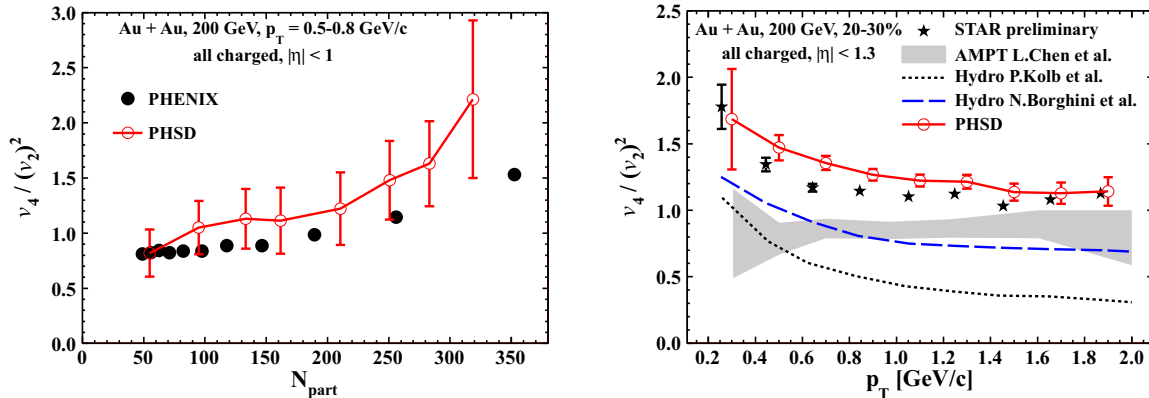


Figure 4. (l.h.s.) Participant number dependence of the $v_4/(v_2)^2$ ratio of charged particles for Au+Au ($\sqrt{s_{NN}} = 200$ GeV) collisions. The experimental data points for $0.5 < p_T < 0.8$ GeV/c are from Ref. [46]. (r.h.s.) Transverse momentum dependence of the ratio $v_4/(v_2)^2$ of charged particles for Au+Au (at $\sqrt{s_{NN}} = 200$ GeV) collisions. The dashed and dot-dashed lines are calculated within the hydrodynamic approaches from Refs. [44] and [45], respectively. The shaded region corresponds to the results from the AMPT model [48]. The experimental data points are from the STAR Collaboration [47].

generated by an intrinsic elliptic flow (at least at high p_T) rather than the fourth order moment of the fluid flow. This is a motivation for studying the ratio $v_4/(v_2)^2$ rather than v_4 alone. As is seen in Fig. 4 (r.h.s.), indeed the ratio calculated within the PHSD model is practically constant in the whole range of $\sqrt{s_{NN}}$ considered but significantly deviates from the ideal fluid estimate of 0.5. In contrast, neglecting dynamical quark-gluon degrees-of-freedom in the HSD model, we obtain a monotonous growth of this ratio.

The dependence of the $v_4/(v_2)^2$ ratio versus the number of participants N_{part} is shown in Fig. 4 for charged particles produced in Au + Au collisions at $\sqrt{s_{NN}} = 200$ GeV. The PHSD results are roughly in agreement with the experimental data points from Ref. [47] but overshoot them for $N_{part} \sim 250$.

As pointed out before, the ratio $v_4/(v_2)^2$ is sensitive to the microscopic dynamics. In this respect we show the transverse momentum dependence of the ratio $v_4/(v_2)^2$ in Fig. 4 for charged particles produced in Au+Au collisions at $\sqrt{s_{NN}} = 200$ GeV (20-30% centrality). The PHSD results are quite close to the experimental data points from Ref. [47], however, overestimate the measurements by up to 20%. The hydrodynamic results – plotted in the same figure – significantly underestimate the experimental data and noticeably depend on viscosity. The partonic AMPT model [48] discussed above also predicts a slightly lower ratio than the measured one, however, being in agreement with both hydrodynamic models for p_T 0.8 GeV/c. Our interpretation of Fig. 4 (r.h.s.) is as follows: the data are not compatible with ideal hydrodynamics and a finite shear viscosity is mandatory (in viscous hydrodynamics) to come closer the experimental observations. The kinetic approaches AMPT and PHSD perform better but either overestimate (in AMPT) or slightly underestimate the scattering rate of soft particles (in PHSD). An explicit study of the centrality dependence of these ratios should provide further valuable information.

3. Conclusions

In summary, relativistic collisions of Au+Au from $\sqrt{s_{NN}} = 5$ to 200 GeV have been studied within the PHSD approach which includes the dynamics of explicit partonic degrees-of-freedom

as well as dynamical local transition rates from partons to hadrons and also the final hadronic scatterings. Whereas earlier studies have been carried out for longitudinal rapidity distributions of various hadrons, their transverse mass spectra and the elliptic flow v_2 as compared to available data at SPS and RHIC energies [19, 20], here we have focussed on the PHSD results for the collective flow coefficients v_2, v_3 and v_4 in comparison to experimental data in the large energy range from the RHIC Beam-Energy-Scan (BES) program as well as different theoretical approaches ranging from hadronic transport models to ideal and viscous hydrodynamics. We mention explicitly that the PHSD model from Ref. [20] has been used for all calculations performed in this study and no tuning (or change) of model parameters has been performed.

We have found that the anisotropic flows – elliptic v_2 , triangular v_3 , hexadecapole v_4 – are reasonably described within the PHSD model in the whole transient energy range naturally connecting the hadronic processes at lower energies with ultrarelativistic collisions where the quark-gluon degrees of freedom become dominant. The smooth growth of the elliptic flow v_2 with the collision energy demonstrates the increasing importance of partonic degrees of freedom. Other signatures of the transverse collective flow, the higher-order harmonics of the transverse anisotropy v_3 and v_4 change only weakly from $\sqrt{s_{NN}} \sim 7$ GeV to the top RHIC energy of $\sqrt{s_{NN}} = 200$ GeV, roughly in agreement with experiment. As shown in this study, this success is related to a consistent treatment of the interacting partonic phase in PHSD whose fraction increases with the collision energy.

The analysis of correlations between particles emitted in ultrarelativistic heavy-ion collisions at large relative rapidity has revealed an azimuthal structure that can be interpreted as solely due to collective flow [49, 50, 51, 52]. This interesting new phenomenon, denoted as triangular flow, results from initial state fluctuations and a subsequent hydrodynamic-like evolution. Unlike the usual directed flow, this phenomenon has no correlation with the reaction plane and should depend weakly on rapidity. Event-by-event hydrodynamics [53] has been a natural framework for studying this triangular collective flow but it has been of interest also to investigate these correlations in terms of the PHSD model. We have found the third harmonics to increase steadily in PHSD with bombarding energy. The coefficient v_3 is compatible with zero for $\sqrt{s_{NN}} > 20$ GeV in case of the hadronic transport model HSD which does not develop ‘ridge-like’ correlations. In this energy range PHSD gives a positive v_3 due to dominant partonic interactions.

Different harmonics can be related to each other and in particular, hydrodynamics predicts that $v_4 \propto (v_2)^2$ [44]. In this work it was noted also that v_4 is largely generated by an intrinsic elliptic flow (at least at high p_T) rather than the fourth order moment of the fluid flow. Indeed, the ratio $v_4/(v_2)^2$ calculated within the PHSD model is approximately constant in the whole considered range of $\sqrt{s_{NN}}$ but significantly deviates from the ideal fluid estimate of 0.5. In contrast, neglecting dynamical quark-gluon degrees-of-freedom in the HSD model, we obtain a monotonous growth of this ratio.

The transverse momentum dependence of the ratio $v_4/(v_2)^2$ at the top RHIC energy has given further interesting information (*cf.* Fig. 4) by comparing the various model results to the data from STAR which are interpreted as follows: the STAR data are not compatible with ideal hydrodynamics and a finite shear viscosity is mandatory (in viscous hydrodynamics) to come closer the experimental ratio observed. The kinetic approaches AMPT and PHSD perform better but either overestimate (in AMPT) or slightly underestimate the scattering rate of soft particles (in PHSD).

We recall that our present PHSD calculations employ ‘naturally’ Glauber type initial state fluctuations which appear compatible with experimental observations up to top RHIC energies. On the other hand one might expect that at LHC energies an initial ‘glasma’ phase might play a sizeable role and that the gluon-field fluctuations - of lower scale - could show up in the Fourier decomposition of the azimuthal angular distribution. It will be interesting to compare the coefficients v_n for high multiplicity pp , $p + Pb$ and $Pb + Pb$ reactions as a function of transverse

momentum p_T (and centrality).

The authors acknowledge financial support through the “HIC for FAIR” framework of the “LOEWE” program.

References

- [1] Mishra A P *et al.* 2008 *Phys. Rev. C* **77** 064902
- [2] Ollitrault J Y 1992 *Phys. Rev. D* **46** 229
- [3] Heinz U and Kolb P 2002 *Nucl. Phys. A* **702** 269
- [4] Shuryak E V 2009 *Prog. Part. Nucl. Phys.* **62** 48
- [5] Shuryak E V 2005 *Nucl. Phys. A* **750** 64
- [6] Gyulassy M and McLerran L 2005 *Nucl. Phys. A* **750** 30
- [7] Peshier A and Cassing W 2005 *Phys. Rev. Lett.* **94** 172301
- [8] Cheng M *et al.* 2008 *Phys. Rev. D* **77** 014511
- [9] Aoki Y *et al.* 2009 *JHEP* **0906** 088
- [10] Adare A *et al.* 2007 *Phys. Rev. Lett.* **98** 172301
- [11] Romatschke P and Romatschke U 2007 *Phys. Rev. Lett.* **99** 172301
- [12] Xu Z, Greiner C and Stöcker H 2008 *Phys. Rev. Lett.* **101** 082302
- [13] Abelev B I *et al.* 2010 *Phys. Rev. C* **81** 024911
- [14] Lacey R A *et al.* 2007 *Phys. Rev. Lett.* **98** 092301
- [15] Aggarwal M M *et al.* 2010 *arXiv:1007.2613*
- [16] Nasim M, Kumar L, Netrakanti P K and Mohanty B 2010 *Phys. Rev. C* **82** 054908
- [17] Konchakovski V P *et al.* 2012 *Phys. Rev. C* **85** 011902
- [18] Konchakovski V P *et al.* 2012 *Phys. Rev. C* **85** 044922
- [19] Cassing W and Bratkovskaya E L 2009 *Nucl. Phys. A* **831** 215
- [20] Bratkovskaya E L, Cassing W, Konchakovski V P and Linnyk O 2011 *Nucl. Phys. A* **856** 162
- [21] Cassing W 2007 *Nucl. Phys. A* **791** 365
- [22] Cassing W 2007 *Nucl. Phys. A* **795** 70
- [23] Cassing W 2009 *Eur. J. Phys.* **168** 3
- [24] Ackermann K H *et al.* 2001 *Phys. Rev. Lett.* **86** 402
- [25] Cassing W *et al.* 1990 *Phys. Rep.* **188** 363
- [26] Bass S A *et al.* 1998 *Prog. Part. Nucl. Phys.* **41** 255
- [27] Bratkovskaya E L, Cassing W and Stöcker H 2003 *Phys. Rev. C* **67** 054905
- [28] Ehehalt W and Cassing W 1996 *Nucl. Phys. A* **602** 449
- [29] Cassing W and Bratkovskaya E L 1999 *Phys. Rep.* **308** 65
- [30] Bratkovskaya E L *et al.* 2004 *Phys. Rev. C* **69** 054907
- [31] Lin Z W and Ko C M 2002 *Phys. Rev. C* **65** 034904
- [32] Lin Z W, Ko C M, Li, B A Zhang B and Pal S 2005 *Phys. Rev. C* **72** 064901
- [33] Cassing W and Bratkovskaya E L 2008 *Phys. Rev. C* **78** 034919
- [34] Mattiello S and Cassing W 2010 *Eur. Phys. J. C* **70** 243
- [35] Demir N and Bass S A 2009 *Phys. Rev. Lett.* **102** 172302
- [36] Ozvenchuk V *et al.*, *arXiv:1212.5393 [hep-ph]*
- [37] Petersen H, Coleman-Smith C, Bass S A and Wolpert R 2011 *J. Phys. G* **38** 045102
- [38] Petersen H and Bleicher M 2010 *Phys. Rev. C* **81** 044906
- [39] Alver B and Roland G 2010 *Phys. Rev. C* **81** 054905
- [40] Adare A *et al.* 2011 *Phys. Rev. Lett.* **107** 252301
- [41] Poskanzer A M and Voloshin S A 1998 *Phys. Rev. C* **58** 1671
- [42] Bilandzic A, Snellings R and Voloshin S A 2011 *Phys. Rev. C* **83** 044913
- [43] Back B B *et al.* 2005 *Phys. Rev. C* **72** 051901
- [44] Kolb P F 2003 *Phys. Rev. C* **68** 031902(R)
- [45] Borghini N and Ollitrault J Y 2006 *Phys. Lett. B* **642** 227
- [46] Gong X Y *et al.* 2011 *J. Phys. G* **38** 124146
- [47] Bai Y *et al.* 2007 *J. Phys. G* **34** S903
- [48] Chen L W, Ko C M and Lin Z W 2004 *Phys. Rev. C* **69** 031901
- [49] Xu J and Ko C M 2011 *Phys. Rev. C* **84** 014903
- [50] Schenke B, Jeon S and Gale C 2011 *Phys. Rev. Lett.* **106** 042301
- [51] Teaney D and Yan L 2011 *Phys. Rev. C* **83** 064904
- [52] Luzum M, Gombeaud C and Ollitrault J Y 2010 *Phys. Rev. C* **81** 054910
- [53] Gardim F G, Grassi F, Hama Y, Luzum M and Ollitrault J Y 2011 *Phys. Rev. C* **83** 064901